Chemical Thermodynamics and Thermal Analysis 21 (2026) 100272

Contents lists available at ScienceDirect

Chemical Thermodynamics and Thermal Analysis

journal homepage: www.elsevier.com/locate/ctta

Experimental and thermodynamic correlation of 4-hydroxycoumarin solubility in aqueous-organic solvent systems (DMSO, ACN, DMF) at eight temperatures

Sintu Ganai [a,*], Bidhan Chandra Mahatha [a,b], Avishek Saha [a,c], Jit Chakraborty [d], Puspal Mukherjee [a], Pratima Mandal [e], Adel Noubigh [f], Sanjay Roy [a,*]

[a] Department of Chemistry, School of Sciences, Netaji Subhas Open University, Kolkata, West Bengal, India
[b] Department of Chemistry, Raniganj Girls' College, Searsole Rajbari, Paschim Bardhaman. W. B, 713358, India
[c] Department of Chemistry, Srikrishna College, Bagula, Nadia, Pin-741502, West Bengal, India
[d] Department of Chemistry, JIS College of Engineering, Kalyani, 741235, Nadia, India
[e] Department of Chemistry, University of Kalyani, Kalyani, 741235, Nadia, India
[f] Center for Scientific Research and Entrepreneurship, Northern Border University, 73213, Arar, Saudi Arabia

ARTICLE INFO

Keywords:
4-Hydroxycoumarin
Solubility
Aqueous–organic binary mixtures
Thermodynamic correlation
Solid–liquid equilibrium

ABSTRACT

The solid–liquid equilibrium solubility of 4-hydroxycoumarin (4-HC) was investigated in pure water, pure organic solvents (DMF, ACN, and DMSO), and their aqueous binary mixtures at eight temperatures ranging from 288.15 to 323.15 K under atmospheric pressure. Solubility measurements were performed using a gravimetric method employing a Shimadzu analytical balance, a thermostatic water bath, a shaker, and a vacuum filtration system. The effects of solvent composition and temperature on 4-HC solubility were systematically examined. The results indicate that solubility is strongly influenced by both factors, with significantly enhanced solubility in aqueous–organic mixtures compared to pure water. The van't Hoff model, the modified Apelblat equation, and the λh model were applied to correlate the experimental data, all showing good agreement with measured values. The resulting insights and model parameters provide useful guidance for optimizing pharmaceutical processes and improving industrial extraction and purification strategies for 4-HC.

1. Introduction

Thermodynamic modeling is essential for predicting, rationalizing, and quantifying the dissolution behavior of drugs in different solvents. The equilibrium solubility of a compound is closely related to the Gibbs free energy associated with solute–solvent interactions [1]. With appropriate models, researchers can evaluate specific solvent–drug interactions and use thermodynamic parameters to describe how combining solvents (co-solvency) influences solubility [2]. Such models are crucial for optimizing formulation design, improving drug absorption, and predicting pharmaceutical processing behavior. By capturing solvent effects governed by dispersion forces, hydrogen bonding, dipole–dipole interactions, and other short-range forces, thermodynamic modeling provides deeper insight into the molecular factors controlling solubility. Measurement of experimental solubility and its correlation with temperature using thermodynamic models have been shown to be essential for formulation development and process optimization of small molecules [3–5]. This understanding also supports improved drug separation [6] and purification processes [7].

4-Hydroxycoumarin ($C_9H_6O_3$; CAS 1076–38–6; IUPAC: 4-Hydroxy-2H-chromen-2-one), abbreviated as 4-HC, is a simple coumarin derivative comprising a lactone ring linked to a phenolic moiety. Chemically, it is moderately polar and capable of hydrogen bonding through its hydroxy group, making it a versatile scaffold for functionalization. Although the parent 4-HC displays only weak biological activity, it serves as an essential precursor for several vitamin K antagonists most notably warfarin and acenocoumarol [8] which inhibit γ-carboxylation of coagulation factors II, VII, IX, and X. Pharmaceutical applications span anticoagulant therapies in human and veterinary medicine [9] and rodenticide formulations. Its significance stems from the delicate balance between efficacy and toxicity, necessitating careful analogue design [10]. In addition, 4-HC derivatives exhibit anti-inflammatory,

* Corresponding authors.
E-mail addresses: sintuganai.sosc@wbnsou.ac.in, sintuganai@gmail.com (S. Ganai), sanjayroyp@gmail.com (S. Roy).

https://doi.org/10.1016/j.ctta.2026.100272
Received 20 December 2025; Received in revised form 17 January 2026; Accepted 24 January 2026
Available online 24 January 2026

antibacterial, and anticancer properties [10–12], highlighting its importance as a privileged chemical scaffold.

Although solubility data are widely available, thermodynamically resolved solubility and solvation energetics of bioactive coumarin derivatives in mixed aqua–organic solvents are still limited. In this study, the solubility of 4-hydroxycoumarin (4-HC) has been measured in pure dimethyl sulfoxide (DMSO), acetonitrile (ACN), and dimethylformamide (DMF), as well as in their aqueous binary mixtures over the temperature range 288.15–323.15 K. The experimental data have been correlated using the van't Hoff, modified Apelblat, and λh models, and the effects of temperature and solvent composition have been analysed in terms of short-range solute–solvent interactions such as dipole–dipole and dispersion forces.

The present work goes beyond routine solubility measurement by systematically examining how solvent polarity, hydrogen-bonding ability, and dielectric constant influence the solvation and dissolution behaviour of 4-HC in DMSO–, DMF–, and ACN–water systems. Since 4-hydroxycoumarin is the core scaffold of warfarin-type anticoagulants [8], its solubility in mixed solvents is directly relevant to formulation, crystallisation, and processing.

The solvent systems were selected to provide a systematic and physically meaningful investigation of solvation behavior of 4-hydroxycoumarin in mixed solvents. ACN, DMF, and DMSO are polar aprotic solvents with markedly different polarity, hydrogen-bond accepting ability, and dielectric constant, making them ideal model solvents for probing solute–solvent interactions and preferential solvation effects when mixed with water. ACN represents a weakly coordinating dipolar aprotic solvent, DMF a moderately coordinating hydrogen-bond acceptor, and DMSO a strongly coordinating solvent. This controlled variation enables a mechanistic understanding of how solvent properties govern solubility and solvation thermodynamics, which is the central objective of this work. Although ACN is toxic and DMF and DMSO have high boiling points, these solvents are previously used in fundamental solubility and thermodynamic studies [13–15] because of their well-defined physicochemical properties and reproducibility.

To the best of our knowledge, no earlier study has reported the temperature-dependent solubility of 4-HC together with a detailed analysis of solute–solvent–temperature interactions in these solvent systems. The present results therefore provide new quantitative insight into solvent-dependent solvation behaviour and temperature effects, and establish reliable solubility benchmarks for 4-HC that are useful for formulation development and process optimisation.

Recent research has provided significant insights into the dissolution behavior of pharmaceutical and bioactive molecules in the presence of co-solvents and additives, creating a strong comparative framework for this work. Trujillo et al. reported the solubility of sulfamethazine in acetonitrile–1-propanol mixtures and demonstrated that dissolution is strongly influenced by composition and system entropy [16]. Cárdenas et al. examined benzocaine in pure and mixed solvents, confirming the suitability of thermodynamic models for accurate solubility prediction in complex media [17]. Shah et al. showed that surfactants and co-solvents markedly alter solubility profiles through mechanisms such as micellization and preferential solvation, thereby affecting the enthalpy–entropy balance of dissolution [18]. Zhang et al. demonstrated that polymeric additives modify the local microenvironment around solutes, influencing solubility and dissolution thermodynamics [19]. Additional studies by Silva et al. [20] and Kumar et al. [21] revealed that aqueous polymer solutions can enhance solubility without chemical modification of the drug. Investigations into coumarin derivatives [22] and selected antibiotics [23] in mixed solvent systems further highlight that strategic tuning of solvent composition can significantly increase solubility. Collectively, these studies underscore the relevance of solvent-engineering strategies and thermodynamic analysis, providing a robust context for the present investigation of 4-HC.

2. Experimental

2.1. Materials

The following purification techniques were used on each experimental co-solvent (DMF, ACN, and DMSO) and solute (4-HC) in order to produce high-purity solvents for carrying out our investigation. The water content of the solvents was determined by Karl Fischer titration using a (MKC-710S, KEM-JAPAN) coulometric titrator with a sensitivity of ±0.1 μg H_2O. Detailed information regarding the chemical compounds used in this investigation is provided in Table 1 (see below).

Acetonitrile (ACN) ([99.9 %, GR, Merck]). First, potassium hydroxide (KOH) from Merck was used to reflux ACN for a number of hours. Fractional distillation was the next step after the refluxing process. During distillation the middle fraction was collected after ensuring complete elimination of ammonia produced during alkali treatment.

Dimethyl sulfoxide (DMSO) [>99.5 %, Spectrochem Pvt. Ltd., India]. It was first dried for three to four days over fused calcium chloride ($CaCl_2$) that was purchased from SRL, India. After that DMSO was decanted after drying and then distilled under low pressure to get rid of any last contaminants.

N, N-Dimethylformamide (DMF) (>99.5 % Spectrochem Pvt. Ltd, India). There were many steps carried out during DMF purification. The DMF was first distilled in an atmosphere of nitrogen (N_2) at low pressure. For a week, the resultant distillate was kept over dry potassium carbonate (K_2CO_3) from SRL, India. The solvent was then decanted and treated with purified phosphorus pentoxide (P_2O_5) that was procured from SRL, India. In order to guarantee high purity, the DMF was lastly redistilled under lower pressure. Karl-Fisher titration was used to measure the water content of the purified solvents, and the result was <0.02 mol dm^{-3}. The distilled samples were kept in tightly sealed bottles within desiccators and went through one more cycle of redistillation before being used.

4-Hydroxycoumarin (>99.0 %, Sigma-Aldrich). The 4-HC was purchased from Sigma-Aldrich. To obtain pure 4-HC, it was subjected to recrystallization from a water–methanol solvent system. The obtained crystallized product was then dried in a vacuum oven for 7 days to remove any residual solvents or impurities.

2.2. Solubility measurement

The analytical gravimetric method [24], which is inherently more accurate than volumetric techniques such as formol titration for solubility measurement, was employed in this study. We used this method to measure the solubility of 4-HC in different aqueous-organic solvent mixtures over a temperature range of 288.15–323.15 K, and the results with error bar representation are shown in Figs. 1–4. The error bar ranges from ± 2 % to ± 5.9 % and these error bars correspond to the combined expanded uncertainty at $k = 2$. Three sets of binary solvent systems-DMSO, ACN, and DMF with water in different weight percentages (0, 20, 40, 60, 80, and 100 wt %) were used in this investigation. To preserve their integrity and avoid contamination, these solvent solutions were meticulously kept in desiccators while not in use. A Shimadzu Analytical Balance with a precision limit of ±0.1 mg was used to make the binary solvents using exact mass dilution procedures. To obtain the required solvent combinations, precise measurements of the required masses of DMF, DMSO, ACN, and water were made. The produced solvent mixtures and an excess of 4-HC were put into properly fitting stoppered glass tubes as part of the experimental apparatus.

The glass tubes were deliberately left partially filled to facilitate efficient mixing during shaking. Initially, an excess amount of solid 4-HC was added to the liquid phase, and the mixtures were shaken thoroughly to enhance solid–solvent interaction, followed by a 2-hour resting period to promote stabilization of the system. Thereafter, magnetic stirring under controlled temperature conditions was applied to ensure continuous mixing and to facilitate the attainment of equilibrium. At

Table 1
Details of Chemical Compounds.

Chemical Name	CAS No.	Source	Initial purity	Purification	Final purity	Analysis method	[d]water percent (wt %)
4-Hydroxy Coumarin	1076–38–6	Sigma Aldrich	≥0.990[a]	Oven dried	≥ 0.995	HPLC[b]	0.05
DMF	68–12–2	Spectrochem	≥ 0.995[a]	Distilling under reduced pressure	≥ 0.995	GC[c]	0.03
DMSO	67–68–5	Spectrochem	≥ 0.995[a]	Distilling under reduced pressure	≥ 0.995[c]	GC[c]	0.05
ACN	75–05–8	Merck	≥ 0.998[a]	Refluxing with KOH & fractional distillation	≥ 0.999	GC[c]	0.03
Water	7732–18–5	Merck	-	Distillation	-	-	-
KOH	1310–58–3	Merck	≥ 0.985[a]	Recrystallization	≥ 0.995	-	0.02
$CaCl_2$	10,043-52–4	SRL	≥ 0.985[a]	None	≥ 0.985	-	0.00
K_2CO_3	584–08–7	SRL	≥ 0.995[a]	None	≥ 0.995	-	0.00
P_2O_5	1314–56–3	SRL	≥ 0.985[a]	None	≥ 0.985	-	0.00

[a] Declared by Supplier.
[b] HPLC means high-performance liquid chromatography.
[c] GC = Gas Chromatography.
[d] Water content was determined by Karl Fischer titration.

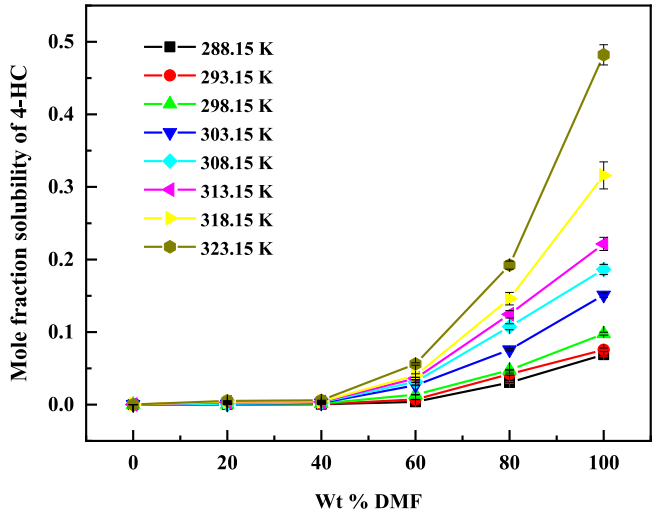

Fig. 1. Solubility alteration of 4-HC in mole fraction scale with weight percent variation of aqueous DMF solutions at different experimental equidistant temperatures. Represented error bar ranges from ± 2 % to ± 5.9 %.

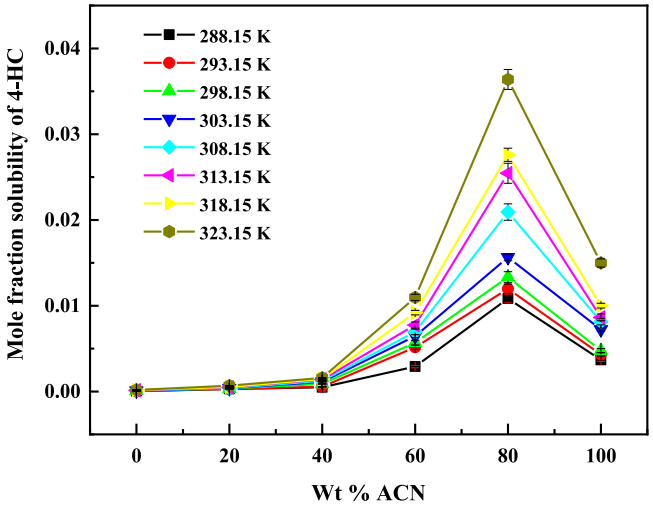

Fig. 3. Solubility alteration of 4-HC in mole fraction scale with weight percent variation of aqueous ACN solutions at different experimental equidistant temperatures. Represented error bar ranges from ± 2.5 % to ± 4.8 %.

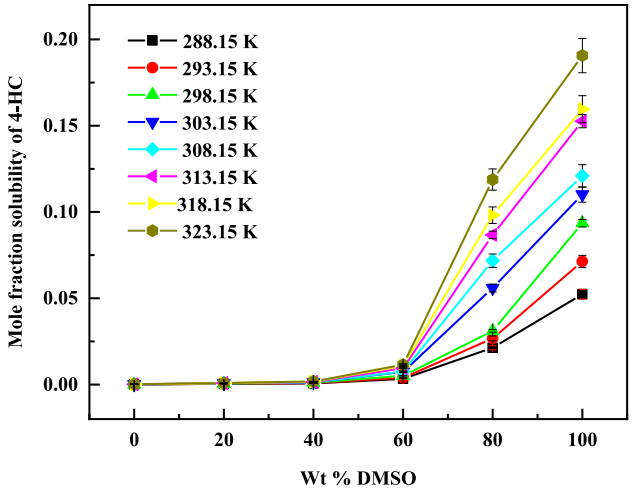

Fig. 2. Solubility alteration of 4-HC in mole fraction scale with weight percent variation of aqueous DMSO solutions at different experimental equidistant temperatures. Represented error bar ranges from ± 2.3 % to ± 4.3 %.

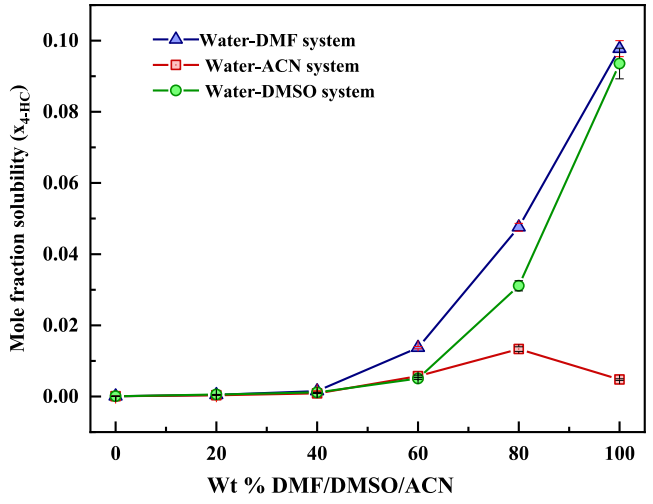

Fig. 4. Comparison of solubility data of 4-HC in pure aqueous and co-solvent mixed solutions at 298.15 K at various weight percent compositions of co-solvent solutions. Represented error bar ranges from ± 2.3 % to ± 4.8 %.

equilibrium, defined as the point where the concentration of 4-HC in the liquid phase remains constant over time, the solubility of 4-HC was determined. Different equilibrium time durations ranging from one to six hours were used to carry out several experiments and a 4-hour equilibration interval consistently ensured that equilibrium was attained, according to a subsequent study [25]. A thermostat–shaker system capable of both low and high temperature ranges was employed as our previous study [26] for temperature-dependent solubility studies. The thermostat demonstrated high accuracy, maintaining temperature within ±0.10 K.

Before being collected for gravimetric analysis [27,28], the sealed glass tubes were left to settle at the appropriate temperature for 6 h. Thereafter, dry pipettes were used to collect 5 mL of each saturated solution. It was then filtered through a 0.22 μm HPLC disposable filter, transferred to a glass vessel, and promptly weighed. After that the solutions were evaporated in a drying oven at 400.15 K for approximately 10–12 h until they were fully dry (since the thermal breakdown temperature of free 4-HC is between 483 and 488 K). Following a 24-hour cooling period in a silica gel-filled dehydrator, the samples were weighed, and the procedure was repeated until a constant weight was reached [29]. On a mole fraction scale, the solubilities of 4-HC in pure water as well as in aqua-organic solvent mixtures were assessed. Each

Table 2
Experimental (x_{exptl}) and calculated (x_{calcd}) mole fraction solubility of 4-HC in different (DMF + water) mixed solvents at temperatures raining from T= (288.15 To 323.15 K) under 0.1 MPa[a].

T/K		van't Hoff equation		Apelblat equation		λh equation	
	$x_{exptl}\times10^3$	$x_{calcd}\times10^3$	RD	$x_{calcd}\times10^3$	RD	$x_{calcd}\times10^3$	RD
w_1 = 0.0000							
288.15	0.0351	0.0419	-0.1928	0.0355	-0.0128	0.0419	-0.1935
293.15	0.0527	0.0539	-0.0236	0.0531	-0.0079	0.0539	-0.0235
298.15	0.0785 (0.0838)[#]	0.0689	0.1221	0.0745	0.0511	0.0689	0.1226
303.15	0.0956 (0.1021)[#]	0.0873	0.0865	0.0984	-0.0297	0.0873	0.0872
308.15	0.1265 (0.1352)[#]	0.1098	0.1319	0.1230	0.0274	0.1097	0.1324
313.15	0.1408 (0.1507)[#]	0.1371	0.0263	0.1459	-0.0364	0.1371	0.0266
318.15	0.1613	0.1699	-0.0536	0.1648	-0.0217	0.1700	-0.0541
323.15	0.1825	0.2093	-0.1468	0.1777	0.0263	0.2096	-0.1486
w_1 = 0.2000							
288.15	0.3051	0.2238	0.2666	0.2571	0.1571	0.2236	0.2672
293.15	0.3383	0.3715	-0.0982	0.3764	-0.1128	0.3714	-0.0980
298.15	0.4471	0.6065	-0.3563	0.5677	-0.2695	0.6067	-0.3567
303.15	0.9274	0.9741	-0.0504	0.8798	0.0513	0.9748	-0.0511
308.15	1.2310	1.5407	-0.2516	1.3989	-0.1364	1.5420	-0.2527
313.15	3.2322	2.4015	0.2570	2.2773	0.2954	2.4032	0.2565
318.15	4.2356	3.6914	0.1285	3.7894	0.1054	3.6918	0.1284
323.15	5.2069	5.5992	-0.0753	6.4348	-0.2358	5.5928	-0.0741
w_1 = 0.4000							
288.15	0.5905	0.6372	-0.0790	0.5289	0.1043	0.6369	-0.0785
293.15	0.7171	0.9247	-0.2894	0.9085	-0.2669	0.9246	-0.2894
298.15	1.5422	1.3251	0.1408	1.4478	0.0612	1.3255	0.1405
303.15	2.3377	1.8766	0.1973	2.1505	0.0801	1.8775	0.1969
308.15	3.0855	2.6277	0.1484	2.9904	0.0308	2.6290	0.1480
313.15	3.8945	3.6401	0.0653	3.9083	-0.0036	3.6411	0.0651
318.15	4.4114	4.9911	-0.1314	4.8191	-0.0924	4.9900	-0.1312
323.15	5.8571	6.7771	-0.1571	5.6254	0.0396	6.7698	-0.1558
w_1 = 0.6000							
288.15	3.7442	5.2690	-0.4072	3.7311	0.0035	5.2464	-0.4012
293.15	7.1457	7.9077	-0.1066	7.6546	-0.0712	7.9164	-0.1079
298.15	13.7132	11.7074	0.1463	13.7977	-0.0062	11.7664	0.1420
303.15	26.6745	17.1100	0.3586	22.0307	0.1741	17.2312	0.3540
308.15	31.6141	24.6997	0.2187	31.3954	0.0069	24.8636	0.2135
313.15	36.0385	35.2405	0.0221	40.2133	-0.1158	35.3449	0.0192
318.15	40.1873	49.7210	-0.2372	46.5988	-0.1595	49.4814	-0.2313
323.15	56.0213	69.4085	-0.2390	49.1498	0.1227	68.1783	-0.2170
w_1 = 0.8000							
288.15	30.4624	30.6376	-0.0058	29.5703	0.0293	30.0551	0.0134
293.15	42.0947	41.1064	0.0235	40.9686	0.0268	40.9859	0.0263
298.15	47.5704	54.6112	-0.1480	55.5394	-0.1675	55.1032	-0.1584
303.15	75.6601	71.8762	0.0500	73.7651	0.0250	73.0178	0.0349
308.15	107.3945	93.7598	0.1270	96.0964	0.1052	95.3281	0.1124
313.15	124.4901	121.2724	0.0258	122.9254	0.0126	122.5578	0.0155
318.15	146.0843	155.5947	-0.0651	154.5594	-0.0580	155.0789	-0.0616
323.15	192.2061	198.0973	-0.0307	191.1961	0.0053	193.0294	-0.0043
w_1 = 1.0000							
288.15	68.8259	59.3794	0.1373	66.0126	0.0409	55.0536	0.2001
293.15	75.6303	80.6969	-0.0670	81.5099	-0.0777	78.8905	-0.0431
298.15	97.7444	108.5449	-0.1105	103.2163	-0.0560	110.5516	-0.1310
303.15	150.9434	144.5823	0.0421	133.8034	0.1136	151.2315	-0.0019
308.15	186.2955	190.8008	-0.0242	177.2766	0.0484	201.5750	-0.0820
313.15	221.5569	249.5735	-0.1265	239.6832	-0.0818	261.3311	-0.1795
318.15	315.9108	323.7065	-0.0247	330.2261	-0.0453	329.1167	-0.0418
323.15	482.1143	416.4940	0.1361	463.0228	0.0396	402.4344	0.1653

[a] Standard uncertainty in temperature u(T) = 0.1 K. The relative standard uncertainty in mole fraction solubility $u_r(x)$=0.03 % (k = 2). If w_1 is the mass fraction of DMF in DMF (w_1) + water (1 − w_1). The relative standard uncertainty of the initial mass fraction of DMF is $u_r(w_1)$ = 0.0002.

[#] for literature report see reference [30].

experiment was repeated three times for every set of binary solutions at every experimental temperature to improve the validity and reliability of our findings. The experimental data exhibited high consistency, with deviations within ± 2 % to ± 5.9 % .

The experimental solubility of 4-HC in an aqueous binary mixture, expressed as its mole fraction (x_{exptl}), is given by the following Eq. (1):

$$x_{exptl} = \frac{\frac{m_{4HC}}{M_{4HC}}}{\frac{m_{4HC}}{M_{4HC}} + \frac{m_W}{M_W} + \frac{m_{OS}}{M_{OS}}} \quad (1)$$

In this context, m_{4HC}, m_W and m_{OS} denote the masses of 4-HC, water, and organic solvents (DMSO/ACN/ or DMF), respectively. The molar masses of these components are represented by M_{4HC}, M_W, and M_{OS}. The experimental solubility values are tabulated in Tables 2–4.

2.3. PXRD and IR spectroscopy analysis:

Powder X-ray diffraction (PXRD) and FTIR spectroscopy were employed to analyze four different samples: pure 4-HC and 4-HC solid obtained by slow evaporation of the filtrate collected through a 0.22 μm HPLC disposable filter from the saturated equilibrium solution (at 298.15 K), for which the solubility was determined in DMF-water, DMSO-water, and ACN-water mixtures. For each solvent system, a 60:40 mass ratio of water to organic solvent (DMSO/ACN/DMF), corresponding to 40 % w/w organic solvent composition was used, and the mixtures were continuously stirred for 12 h prior to attain saturated solid-liquid equilibrium at 298.15 K. It was the filtered through a 0.22 μm HPLC disposable filter and the filtrate was slowly evaporated to dryness in open air. Then the residual solids were kept in a vacuum desiccator for 24 h prior to analysis. PXRD measurements were carried out on a Bruker D8 X-ray diffractometer using Cu-Kα radiation (λ = 0.15405 nm). FTIR spectra were recorded using an Agilent Cary 630 FTIR spectrometer equipped with a diamond ATR accessory.

PXRD data were collected over a 2θ range of 5°–90° at a scanning rate of 4° min^{-1} under standard ambient conditions. As no significant diffraction peaks were observed above 50° (2θ), the displayed range in Fig. 5 has been limited to the low-angle region, which contains the most relevant information for phase identification.

PXRD was used as the primary technique to verify phase identity and crystallinity of the residual solids. FT-IR spectroscopy was employed as a complementary method to confirm that no chemical transformation or strong solvent–solute adduct formation occurred during dissolution and recrystallisation in the mixed solvents. The FT-IR spectra of the recovered solids (Figure S1) show no new bands or significant shifts relative to pure 4-hydroxycoumarin.

The combined PXRD and FT-IR results therefore confirm that the solid recovered after equilibration remains chemically and structurally identical to 4-HC, indicating that no polymorphic or chemical modification occurred during the solubility experiments. The PXRD patterns are presented in Fig. 5.

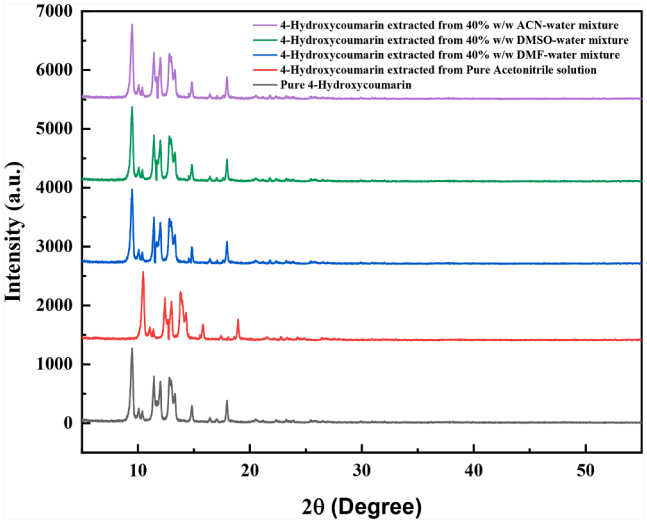

Fig. 5. PXRD patterns of (a) pure solid 4-HC (black trace) & residual solid of 4-HC obtained by slow evaporation of the filtrate collected through a 0.22 μm HPLC disposable filter from the saturated equilibrium solution at 298.15 K in (b) pure acetonitrile solvent (red trace) (c) 40 % w/w DMF-water mixture (blue trace), and (d) 40 % w/w DMSO-water mixture (green trace), (e) 40 % w/w acetonitrile-water mixture (violet trace).

3. Result and discussion

3.1. Analysis of solubility data

In this study, the mole fraction solubilities of 4-HC were determined in pure solvents (water, DMSO, ACN, and DMF) as well as in binary mixtures of DMSO + water, ACN + water, and DMF + water over the temperature range of 288.15–323.15 K. In the literature, only a single source is available [30] for the saturated equilibrium solubility of 4-HC in pure water only at four temperatures within the temperature range 298.15 K to 313.15 K. Our experimentally determined solubility values in pure water were found to deviate 6–7 % in these four temperatures than the reported literature data and the comparison is shown in Fig. 6. It is noteworthy that, in the present study, a wider range of temperatures (288.15–323.15 K) were used for evaluating the equilibrium solubility compared to earlier studies [30]. The observed deviation is likely attributable to differences in experimental methodology, source of chemicals, solid-phase forms, and minor variations in water content within the solvent systems. To confirm the reliability of our solubility data, we repeated our experiments three times and found almost consistent results. The full set of experimental results and their theoretical co-relations are presented in Tables 2–4.

A slight scatter in solubility data was observed, mainly in DMSO–-water and ACN–water mixtures at water-rich compositions. This behavior arises from the strongly non-ideal behavior of water–polar aprotic solvent mixtures. Preferential solvation, micro-heterogeneity, and temperature-dependent solvent structure in DMF–water and ACN–water systems can cause abrupt changes in the local solvation environment of 4-HC, leading to segmented or non-smooth solubility curves. The DMF–water system displayed smaller deviations due to its lower viscosity. Overall, all data points lie within the expanded uncertainty ranges from ±2 % to ±5.9 % (expanded, $k = 2$), confirming the reproducibility and reliability of the experimental solubilities for 4-HC

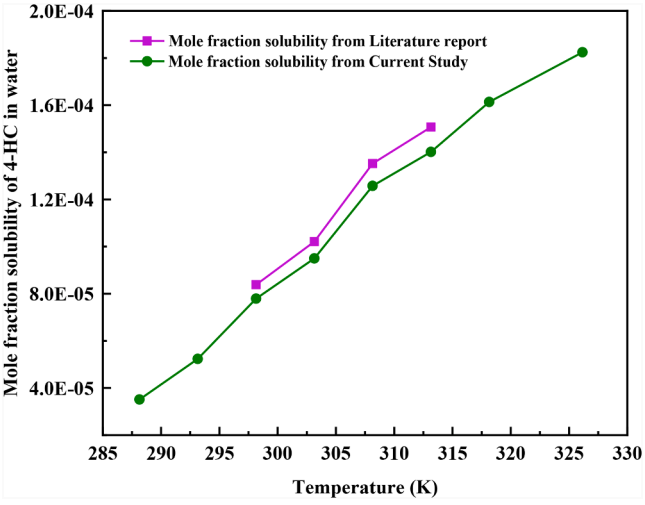

Fig. 6. Comparison of solubility data with available literature report [30] for 4-HC in pure water at various equilibrium temperatures.

Table 3
Experimental (x_{exptl}) and calculated (x_{calcd}) mole fraction solubility of 4-HC in different (DMSO + water) mixed solvents at temperatures raining from T= (288.15 To 323.15 K) under 0.1 MPa[a].

T/K		van't Hoff equation		Apelblat equation		λh equation	
	$x_{exptl} \times 10^3$	$x_{calcd} \times 10^3$	RD	$x_{calcd} \times 10^3$	RD	$x_{calcd} \times 10^3$	RD
w_1 = 0.0000							
288.15	0.0351	0.0419	-0.1928	0.0355	-0.0128	0.0419	-0.1935
293.15	0.0527	0.0539	-0.0236	0.0531	-0.0079	0.0539	-0.0235
298.15	0.0785 (0.0838)[#]	0.0689	0.1221	0.0745	0.0511	0.0689	0.1226
303.15	0.0956 (0.1021)[#]	0.0873	0.0865	0.0984	-0.0297	0.0873	0.0872
308.15	0.1265 (0.1352)[#]	0.1098	0.1319	0.1230	0.0274	0.1097	0.1324
313.15	0.1408 (0.1507)[#]	0.1371	0.0263	0.1459	-0.0364	0.1371	0.0266
318.15	0.1613	0.1699	-0.0536	0.1648	-0.0217	0.1700	-0.0541
323.15	0.1825	0.2093	-0.1468	0.1777	0.0263	0.2096	-0.1486
w_1 = 0.2000							
288.15	0.4280	0.4512	-0.0543	0.4161	0.0278	0.4557	-0.0648
293.15	0.4875	0.5071	-0.0402	0.5033	-0.0323	0.5092	-0.0445
298.15	0.5633	0.5677	-0.0079	0.5900	-0.0475	0.5675	-0.0074
303.15	0.7080	0.6332	0.1057	0.6719	0.0510	0.6310	0.1088
308.15	0.7506	0.7037	0.0625	0.7445	0.0082	0.7001	0.0673
313.15	0.8044	0.7794	0.0310	0.8040	0.0006	0.7753	0.0362
318.15	0.8389	0.8606	-0.0258	0.8475	-0.0102	0.8570	-0.0215
323.15	0.8725	0.9472	-0.0857	0.8734	-0.0011	0.9459	-0.0842
w_1 = 0.4000							
288.15	0.6381	0.7217	-0.1311	0.6493	-0.0176	0.7250	-0.1362
293.15	0.8044	0.8424	-0.0472	0.8340	-0.0368	0.8435	-0.0487
298.15	1.1322	0.9781	0.1362	1.0285	0.0917	0.9771	0.1370
303.15	1.2549	1.1300	0.0995	1.2209	0.0271	1.1274	0.1016
308.15	1.3369	1.2995	0.0279	1.3985	-0.0461	1.2958	0.0307
313.15	1.4600	1.4878	-0.0191	1.5491	-0.0610	1.4842	-0.0166
318.15	1.6658	1.6961	-0.0182	1.6627	0.0019	1.6945	-0.0173
323.15	1.7896	1.9257	-0.0761	1.7326	0.0319	1.9289	-0.0778
w_1 = 0.6000							
288.15	3.3713	3.4345	-0.0188	3.1847	0.0553	3.4390	-0.0201
293.15	3.8727	4.2215	-0.0901	4.1914	-0.0823	4.2231	-0.0905
298.15	5.0527	5.1529	-0.0198	5.3412	-0.0571	5.1515	-0.0196
303.15	7.3728	6.2486	0.1525	6.6035	0.1043	6.2443	0.1531
308.15	7.5323	7.5301	0.0003	7.9354	-0.0535	7.5238	0.0011
313.15	9.4921	9.0205	0.0497	9.2843	0.0219	9.0144	0.0503
318.15	10.8631	10.7447	0.0109	10.5930	0.0249	10.7427	0.0111
323.15	11.4811	12.7293	-0.1087	11.8035	-0.0281	12.7380	-0.1095
w_1 = 0.8000							
288.15	21.3467	21.0310	0.0148	19.6360	0.0801	20.8195	0.0247
293.15	26.7776	28.0365	-0.0470	27.8550	-0.0402	28.0158	-0.0462
298.15	31.0889	37.0169	-0.1907	38.2445	-0.2302	37.2392	-0.1978
303.15	55.9463	48.4279	0.1344	50.9218	0.0898	48.8969	0.1260
308.15	71.7871	62.8065	0.1251	65.8716	0.0824	63.4188	0.1166
313.15	86.7361	80.7807	0.0687	82.9257	0.0439	81.2354	0.0634
318.15	98.1374	103.0801	-0.0504	101.7565	-0.0369	102.7471	-0.0470
323.15	118.7884	130.5468	-0.0990	121.8869	-0.0261	128.2841	-0.0799
w_1 = 1.0000							
288.15	52.3838	58.4802	-0.1164	53.9427	-0.0298	57.9691	-0.1066
293.15	71.3239	70.9284	0.0055	70.3881	0.0131	70.9286	0.0055
298.15	93.5650	85.4713	0.0865	88.8164	0.0508	85.9753	0.0811
303.15	110.1123	102.3643	0.0704	108.5952	0.0138	103.2533	0.0623
308.15	120.9021	121.8806	-0.0081	128.9099	-0.0662	122.8726	-0.0163
313.15	152.6228	144.3114	0.0545	148.8312	0.0248	144.8991	0.0506
318.15	159.5615	169.9655	-0.0652	167.4002	-0.0491	169.3453	-0.0613
323.15	190.6573	199.1691	-0.0446	183.7146	0.0364	196.1639	-0.0289

[a] Standard uncertainty in temperature u(T) = 0.1 K. The relative standard uncertainty in mole fraction solubility $u_r(x)$=0.025 % (k = 2). If w_1 is the mass fraction of DMSO in DMSO (w_1) + water (1 − w_1). The relative standard uncertainty of the initial mass fraction of DMSO is $u_r(w_1)$ = 0.0002.
[#] for literature report see reference [30].

across the studied binary solvent mixtures.

As shown in Fig. 1–4, the solubilities of 4-HC in the experimental binary solvent mixtures increases as the absolute temperature rises. In general, adding organic solvents like DMSO, ACN, or DMF boosts the solubility of 4-HC. In mixtures such as DMSO + water, ACN + water, and DMF + water, a higher proportion of the organic solvent leads to greater solubility, this trend is clearly supported by the data in Tables 2–4 and Fig. 7. Temperature has a more pronounced effect on solubility in DMF-water and DMSO-water mixtures compared to ACN-water mixture. Also, at the same solvent ratios, 4-HC tends to be more soluble in DMF-water than in DMSO-water or ACN-water mixture.

Analysis of the experimental data (Tables 2–4 and Figs. 1–4) reveals a key finding: the equilibrium solubility of 4-hydroxycoumarin (4-HC) consistently increases with temperature across all solvent systems, reflecting the endothermic nature of its dissolution process. This behaviour arises because increasing temperature raises molecular kinetic energy [31], enhancing solvent mobility and promoting more effective disruption of solute–solute and solvent–solvent structures. Consequently, specific solute–solvent interactions are strengthened, resulting in higher solubility.

In pure solvents, the solubility trend follows the order **DMF > DMSO > ACN > H_2O**. This behaviour is governed by solvent polarity,

Table 4
Experimental (x_{exptl}) and calculated (x_{calcd}) mole fraction solubility of 4-HC in different (ACN + water) mixed solvents at temperatures raining from T= (288.15 To 323.15 K) under 0.1 MPa[a].

T/K		van't Hoff equation		Apelblat equation		λh equation	
	$x_{exptl} \times 10^3$	$x_{calcd} \times 10^3$	RD	$x_{calcd} \times 10^3$	RD	$x_{calcd} \times 10^3$	RD
w_1 = 0.0000							
288.15	0.0351	0.0419	-0.1928	0.0355	-0.0128	0.0419	-0.1935
293.15	0.0527	0.0539	-0.0236	0.0531	-0.0079	0.0539	-0.0235
298.15	0.0785 (0.0838)[#]	0.0689	0.1221	0.0745	0.0511	0.0689	0.1226
303.15	0.0956 (0.1021)[#]	0.0873	0.0865	0.0984	-0.0297	0.0873	0.0872
308.15	0.1265 (0.1352)[#]	0.1098	0.1319	0.1230	0.0274	0.1097	0.1324
313.15	0.1408 (0.1507)[#]	0.1371	0.0263	0.1459	-0.0364	0.1371	0.0266
318.15	0.1613	0.1699	-0.0536	0.1648	-0.0217	0.1700	-0.0541
323.15	0.1825	0.2093	-0.1468	0.1777	0.0263	0.2096	-0.1486
w_1 = 0.2000							
288.15	0.2930	0.2706	0.0765	0.2935	-0.0017	0.2749	0.0617
293.15	0.3041	0.3072	-0.0104	0.3096	-0.0182	0.3098	-0.0188
298.15	0.3473	0.3474	-0.0001	0.3342	0.0378	0.3480	-0.0020
303.15	0.3675	0.3912	-0.0644	0.3686	-0.0030	0.3900	-0.0613
308.15	0.4028	0.4388	-0.0894	0.4147	-0.0297	0.4359	-0.0824
313.15	0.4905	0.4904	0.0003	0.4754	0.0308	0.4862	0.0089
318.15	0.5350	0.5462	-0.0209	0.5546	-0.0366	0.5411	-0.0115
323.15	0.6695	0.6062	0.0945	0.6576	0.0178	0.6011	0.1022
w_1 = 0.4000							
288.15	0.4864	0.5341	-0.0980	0.4558	0.0629	0.5359	-0.1018
293.15	0.5521	0.6481	-0.1739	0.6385	-0.1565	0.6489	-0.1754
298.15	0.8811	0.7814	0.1132	0.8425	0.0438	0.7810	0.1136
303.15	1.1219	0.9362	0.1655	1.0513	0.0629	0.9348	0.1668
308.15	1.2344	1.1151	0.0966	1.2449	-0.0085	1.1129	0.0984
313.15	1.3983	1.3209	0.0553	1.4033	-0.0036	1.3185	0.0571
318.15	1.4599	1.5563	-0.0661	1.5105	-0.0347	1.5547	-0.0650
323.15	1.5833	1.8244	-0.1523	1.5569	0.0166	1.8255	-0.1530
w_1 = 0.6000							
288.15	2.9054	3.6467	-0.2551	3.3554	-0.1549	3.6625	-0.2606
293.15	5.1615	4.3399	0.1592	4.3059	0.1658	4.3478	0.1577
298.15	5.6988	5.1348	0.0990	5.3421	0.0626	5.1341	0.0991
303.15	6.4576	6.0417	0.0644	6.4212	0.0056	6.0327	0.0658
308.15	6.9638	7.0713	-0.0154	7.4921	-0.0759	7.0555	-0.0132
313.15	7.7486	8.2349	-0.0628	8.5009	-0.0971	8.2158	-0.0603
318.15	9.1971	9.5441	-0.0377	9.3956	-0.0216	9.5278	-0.0360
323.15	10.9704	11.0111	-0.0037	10.1314	0.0765	11.0071	-0.0033
w_1 = 0.8000							
288.15	10.8355	9.8304	0.0928	10.5647	0.0250	9.8521	0.0908
293.15	11.9664	11.9444	0.0018	12.0261	-0.0050	11.9623	0.0003
298.15	13.3314	14.4183	-0.0815	13.9330	-0.0451	14.4301	-0.0824
303.15	15.6315	17.2970	-0.1065	16.4090	-0.0497	17.2995	-0.1067
308.15	20.9189	20.6282	0.0139	19.6220	0.0620	20.6177	0.0144
313.15	25.4470	24.4630	0.0387	23.7993	0.0647	24.4348	0.0398
318.15	27.5953	28.8556	-0.0457	29.2497	-0.0600	28.8041	-0.0438
323.15	36.3793	33.8635	0.0692	36.3930	-0.0004	33.7819	0.0714
w_1 = 1.0000							
288.15	3.6778	3.5289	0.0405	3.6470	0.0084	3.5416	0.0370
293.15	4.3218	4.3489	-0.0063	4.3625	-0.0094	4.3575	-0.0083
298.15	4.7660	5.3220	-0.1167	5.2394	-0.0993	5.3252	-0.1173
303.15	7.2206	6.4697	0.1040	6.3157	0.1253	6.4662	0.1045
308.15	8.1465	7.8152	0.0407	7.6386	0.0623	7.8043	0.0420
313.15	8.6439	9.3837	-0.0856	9.2664	-0.0720	9.3655	-0.0835
318.15	10.0068	11.2023	-0.1195	11.2720	-0.1264	11.1781	-0.1171
323.15	14.9796	13.3004	0.1121	13.7456	0.0824	13.2734	0.1139

[a] Standard uncertainty in temperature u(T) = 0.1 K. The relative standard uncertainty in mole fraction solubility $u_r(x)$=0.025 % (k = 2). If w_1 is the mass fraction of ACN in ACN (w_1) + water (1 − w_1). The relative standard uncertainty of the initial mass fraction of ACN is $u_r(w_1)$ = 0.0002.
[#] for literature report see reference [30].

hydrogen-bonding capacity, and molecular interaction patterns. Although DMSO is more polar (ε ≈ 47, μ ≈ 4.0 D) than DMF (ε ≈ 37, μ ≈ 3.8 D), polarity alone does not dictate solubility; the accessibility of interaction sites is more decisive. DMF, with its less sterically hindered carbonyl oxygen and resonance-stabilized amide group, provides stronger hydrogen-bond acceptance and dipole–dipole stabilization with both the hydroxyl and lactone functionalities of 4-HC, leading to the highest solubility. In contrast, DMSO, despite its high polarity, contains a sterically bulky sulfoxide group that reduces its ability to stabilize the aromatic heterocyclic system of 4-HC, resulting in slightly lower solubility than DMF. Acetonitrile (ACN), a polar aprotic solvent containing a nitrile group, stabilizes dipoles but is a comparatively weak hydrogen-bond acceptor. This limits its ability to solvate aromatic heterocycles with hydroxyl groups, yielding moderate solubility. Water, despite its strong hydrogen-bonding network, poorly accommodates hydrophobic aromatic rings, resulting in the lowest solubility among the investigated solvents.

Across all compositions and temperatures, the DMF-water system exhibits the highest solubility of 4-HC, while the ACN-water system shows the lowest. At each temperature, the solubility trend in binary aqueous–organic mixtures increases in the order: water + ACN < water + DMSO < water + DMF, correlating with increasing mole fraction of

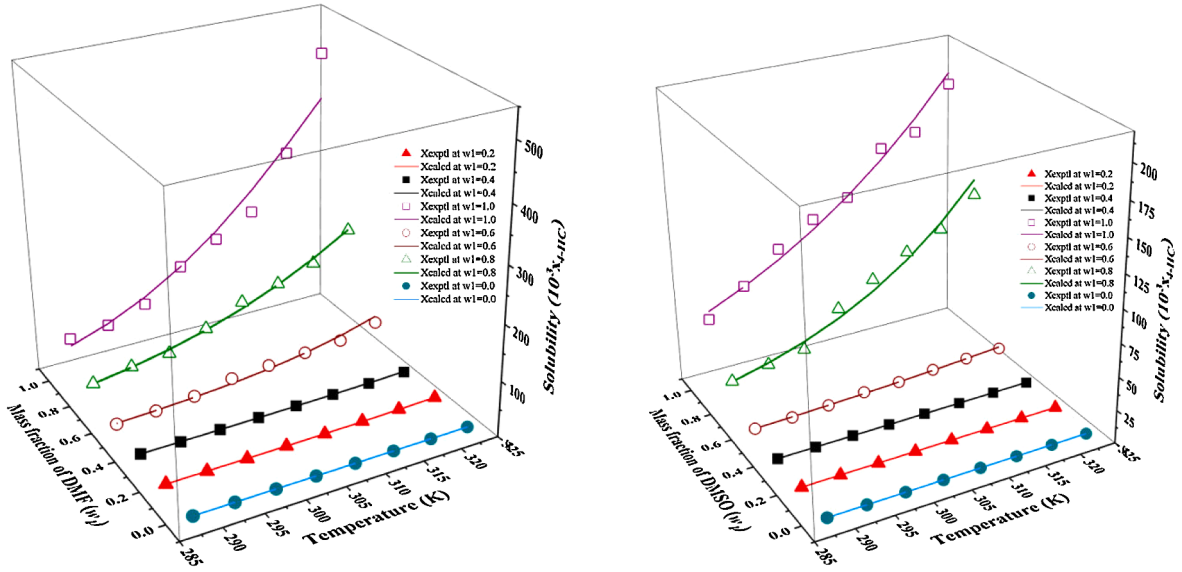

(a) experiment *vs* λh fit

(b) experiment *vs* van't Hoff fit

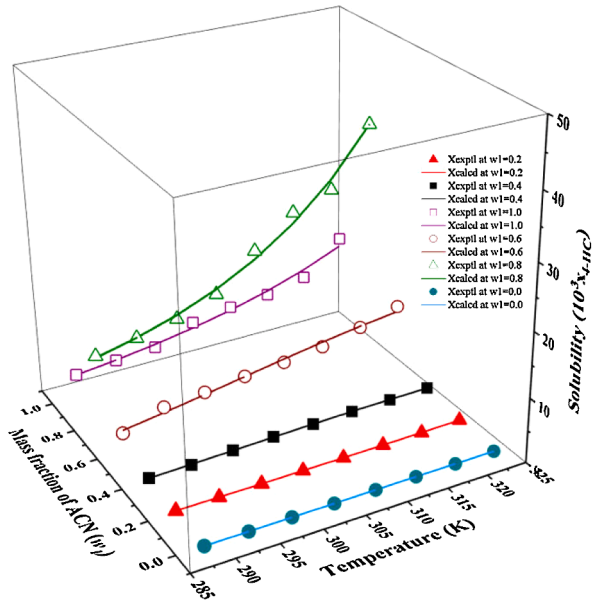

(c) experiment *vs* modified Apelblat fit

Fig. 7. Mole fraction solubilities of 4-HC in three binary solvent mixtures at various temperatures at various mass fraction compositions of co-solvent; ●, $w_1 = 0.0$; ▲, $w_1 = 0.2$; ■, $w_1 = 0.4$; ∘, $w_1 = 0.6$; Δ, $w_1 = 0.8$; □, $w_1 = 1.0$; solid line denotes the corresponding solubility calculated with (a) DMF–water: λh equation (b) DMSO–water: van't Hoff equation and (c) ACN–water: modified Apelblat equation.

organic solvent. These differences arise from the balance between solvent polarity, hydrogen-bonding ability, and hydrophobic stabilization of the aromatic moiety, all modulated by water content in the mixture.

A prominent observation is that increasing water content significantly suppresses the solubility of 4-HC, demonstrating a clear anti-solvent effect. Water, with its high dielectric constant ($\varepsilon \approx 78$ at 298 K) and strong hydrogen-bonding capacity, effectively solvates the hydroxyl group but fails to stabilize the hydrophobic aromatic core, thereby limiting overall solubility. Greater solute–solvent compatibility in organic solvents (DMF, DMSO, ACN) explains their enhanced solubilization efficiency. The dipole moments of 4-HC, DMSO, DMF, ACN, and water are 4.849 D, 3.90 D, 3.82 D, 3.45 D, and 1.83 D, respectively [32–34], supporting stronger dipole–dipole interactions with organic solvents and weaker interactions with water, especially upon dilution. Molecular size also influences solubility: larger solvent molecules tend to show enhanced polarizability and stronger dispersion interactions with the aromatic moiety of 4-HC. The sizes of 4-HC, DMF, DMSO, ACN, and water are 4.48 Å, 4.98 Å, 4.91 Å, 4.12 Å, and 2.74 Å, respectively [33–35]. Generally, larger size enhances polarizability, which in turn promotes dispersion and soft-soft interactions between organic solvents and the aromatic moiety of 4-HC. DMF and 4-HC interact particularly effectively due to their comparable size, explaining its higher solubility in DMF compared to DMSO and the generally poor solubility in water. Dimerization tendencies of the solvents further clarify solubility variations: DMF and DMSO can form dimers, though with differing stability, in the order $(DMF)_2 > (DMSO)_2$ [36,37]. More stable DMF dimers can still effectively interact with 4-HC, contributing to its higher solubility. Importantly, no significant chemical reactions involving 4-HC occurred

in any of the organic solvent compositions in mixed systems, as confirmed by UV–VIS tests.

A notable feature was observed in the ACN–water system, where the solubility of 4-HC increased up to ~80 wt % ACN and then declined toward pure ACN. ACN is a weaker base than water, DMF, and DMSO [25,38], and its lower hydrogen-bond-accepting ability limits its capacity to solvate 4-HC in ACN-rich mixtures. Consequently, 4-HC experiences poor solvation in aqueous ACN systems, leading to reduced solubility at higher ACN content. In addition, ACN exhibits phobic behaviour toward both positive and negative charges [39], further diminishing solvation efficiency in ACN-water mixtures. Thus, both limited hydrogen-bond acceptance and charge-phobicity contribute to the relatively poor solubility of 4-HC in ACN compared to the other solvents investigated. Furthermore, ACN can dimerize at high concentrations, reducing the availability of free solvent molecules for effective solute–solvent interactions. As a result, ACN behaves as an anti-solvent for 4-HC at high weight fractions, whereas water becomes the more effective solvating component. The observed solubility maximum at ~80 wt % ACN reflects a classic co-solvent effect: at this composition, the mixture polarity and hydrogen-bonding characteristics optimally match the amphiphilic nature of 4-HC. ACN disrupts the strong water–water hydrogen-bond network, lowering the hydrophobic penalty, while sufficient water molecules remain to provide hydrogen-bond donor and acceptor sites for stabilizing the hydroxyl and lactone groups of 4-HC. Preferential solvation by ACN-rich microenvironments around 4-HC at these intermediate compositions lowers the solute's activity coefficient, enhancing its apparent solubility. Beyond ~80 wt % ACN, the solvent mixture loses hydrogen-bond donor capacity, and solvation of polar sites becomes less effective, leading to the observed decrease in solubility.

3.2. Solubility correlation and calculation

Experimental data on the solubility of 4-HC in pure as well as binary mixed solvents have been correlated using three models: the van't Hoff model, the modified Apelblat equation, and the λh equation. These models combine several thermodynamic parameters to predict trends of solubility for understanding the dissolution characteristics of drugs. To establish the validity of these correlations, we have calculated the relative average deviation (RAD), root mean square deviation (RMSD), and the relative deviations (RD) by comparing them with the predicted values by these models. The smaller RAD and RMSD values reflect closer agreement between the calculated values by the models and the experimental data, thus demonstrating the capability of these models to follow closely the sophisticated solvation interactions. Definitions of RAD, RMSD, and RD are given by Eqs.. (2), (3), and (4), respectively.

$$\mathrm{RAD} = \frac{1}{\mathrm{n}} \times \sum_{i=1}^{\mathrm{n}} \left| \frac{\mathrm{x_{exptl}} - \mathrm{x_{calcd}}}{\mathrm{x_{exptl}}} \right| \tag{2}$$

$$\mathrm{RMSD} = \left[\frac{1}{\mathrm{n}} \times \sum_{i=1}^{\mathrm{n}} \left(\mathrm{x_{calcd}} - \mathrm{x_{exptl}} \right)^2 \right]^{\frac{1}{2}} \tag{3}$$

$$\mathrm{RD} = \frac{\mathrm{x_{exptl}} - \mathrm{x_{calcd}}}{\mathrm{x_{exptl}}} \tag{4}$$

'n' refers to the total number of data points collected during the experiments. The terms x_{exptl} represent the mole fraction solubilities obtained from calculations and experimental measurements, respectively.

3.2.1. The van't hoff model

The van't Hoff equation [40,41] shows a straightforward linear relationship between the natural logarithm of a solute's mole fraction solubility and the inverse of the absolute temperature (1/T) in a solution. It's represented by the following Eq. (5).

$$\ln x = a + \frac{b}{T/K} \tag{5}$$

In this equation, x stands for the mole fraction of 4-HC in the solvent mixture, while T refers to the absolute temperature in Kelvin. The constants a and b are obtained by fitting the experimental solubility data using regression analysis.

3.2.2. The modified apelblat equation

The modified Apelblat equation [42–44] is used to simulate how the solubility of 4-HC changes with temperature in both pure solvents and binary mixtures. This semi-empirical model takes into account non-ideal solution behavior and the effect of temperature on the solvation process and is expressed mathematically in Eq. (6):

$$\ln x = A + \frac{B}{\frac{T}{K}} + C \ln(T/K) \tag{6}$$

Here, A, B, and C are constants derived from regression analysis, and T stands for the absolute temperature in Kelvin (K). A and B help account for how the solute's activity coefficient changes when the solution behaves non-ideally. On the other hand, C reflects how the solute's enthalpy of fusion affects its solubility as the temperature changes.

3.2.3. The λh equation

The Buchowski-Ksiazczak λh equation was used to describe how solubility changes with temperature during the solute's dissolution. In this study, the experimental solubility data were examined using the λh model [45,46], which offers a semi-empirical approach to understanding the influence of temperature on solute solubility in different solvent systems.

$$\ln\left[1 + \frac{\lambda(1-x)}{x}\right] = \lambda h \left[\frac{1}{\left(\frac{T}{K}\right)} - \frac{1}{\left(\frac{T_m}{K}\right)}\right] \tag{7}$$

In the Eq. (7), T_m represents the solute's melting point, while λ and *h* are parameters obtained by fitting experimental solubility data. The melting point (Tm) of 4-hydroxycoumarin (4-HC) used in the λh-model was taken as 213 °C (486.15 K), based on the supplier's specification (Sigma-Aldrich, CAS No 1076–38–6). The λ value indicates how much the system deviates from ideal solution behavior DMSO during dissolution, and *h* relates to the excess enthalpy of the solution, capturing the energy involved in solute-solvent interactions. Together, these parameters help explain the thermodynamic forces that influence solubility as the temperature changes.

In this study, a MATLAB-based computational approach was used to match the experimental solubility data with three thermodynamic models (Eqs. (5)–7). The solubility values predicted by these models are presented in Tables 2–4. The relative deviation (RD) values calculated from the experimental data are presented in Tables 2–4. The relative deviation (RD) between experimental and calculated mole-fraction solubilities was evaluated for all three models. The RD values range from near zero to approximately 0.55, depending on temperature and solvent composition. Larger deviations are observed mainly in intermediate DMF-water and ACN-water mixtures, reflecting the strong non-ideality and preferential solvation effects that are characteristic of mixed aqueous–aprotic solvent systems. Such behavior is well documented and indicates limitations of classical semi-empirical models rather than experimental inconsistency. Despite local deviations, all three models satisfactorily reproduce the overall temperature and composition dependence of the solubility

Additionally, Tables 5–7 present the optimized model parameters along with the root-mean-square deviation (RMSD) and average relative deviation (RAD %) values. These metrics help evaluate how well each model captures the solubility behavior of 4-HC across the different solvent systems.

Table 5
Values of parameters obtained using solubility models for 4-HC in different (DMF + water) mixed solvents.

x_{DMF}	van't Hoff equation				
	a/K	b	RMSD×10^3	RAD×10^2	
0.00	4.78	-4281.08	0.01	9.80	
0.20	21.32	-8566.19	0.40	18.55	
0.40	14.47	-6289.78	0.47	15.11	
0.60	18.56	-6859.10	2.55	16.65	
0.80	13.75	-4965.81	6.95	5.95	
1.00	15.16	-5182.35	26.09	8.35	
x_{DMF}	λh equation				
	λ	h	RMSD×10^3	RAD×10^2	
0.00	0.02	247,764.67	0.005	9.86	
0.20	41.30	207.74	0.40	18.56	
0.40	4.70	1340.36	0.47	15.07	
0.60	103.77	67.41	2.42	21.08	
0.80	66.61	81.50	2.15	5.33	
1.00	576.35	11.29	11.66	10.56	
x_{DMF}	Apelblat equation				
	A	B/K	C	RMSD×10^3	RAD×10^2
0.00	1177.30	-57,487.38	-174.46	0.00	2.67
0.20	-975.37	36,661.53	148.30	0.58	17.05
0.40	1349.03	-66,849.19	-198.57	0.20	8.49
0.60	2492.72	-119,131.06	-368.13	1.41	8.25
0.80	267.82	-16,495.01	-37.80	5.83	5.37
1.00	-743.67	29,251.49	112.90	12.97	6.29

Table 6
Values of parameters obtained using solubility models for 4-HC in different (DMSO + water) mixed solvents.

x_{DMSO}	van't Hoff equation				
	a/K	b	RMSD×10^3	RAD×10^2	
0.00	4.78	-4281.08	0.01	9.80	
0.20	-0.86	-1972.82	0.04	5.16	
0.40	1.83	-2611.01	0.09	6.94	
0.60	6.42	-3485.27	0.63	5.63	
0.80	12.99	-4857.27	6.82	9.12	
1.00	8.48	-3260.29	7.19	5.64	
x_{DMSO}	λh equation				
	λ	h	RMSD×10^3	RAD×10^2	
0.00	0.02	247,764.67	0.005	9.86	
0.20	0.005	372,530.48	0.02	5.44	
0.40	0.02	106,296.98	0.03	7.07	
0.60	0.45	7647.99	0.22	5.69	
0.80	30.20	170.09	2.17	8.77	
1.00	10.18	355.58	2.26	5.16	
x_{DMSO}	Apelblat equation				
	A	B/K	C	RMSD×10^3	RAD×10^2
0.00	1177.30	-57,487.38	-174.46	0.00	2.67
0.20	580.39	-28,348.44	-86.48	0.02	2.23
0.40	759.25	-36,981.16	-112.70	0.06	3.93
0.60	547.50	-28,038.16	-80.51	0.39	5.34
0.80	504.80	-27,174.41	-73.18	4.37	7.87
1.00	587.22	-29,522.25	-86.11	5.20	3.55

The fitting quality of the van't Hoff, λh, and modified Apelblat models was evaluated using RAD and RMSD values. In DMSO–water mixtures, the maximum RAD values were 9.80 %, 9.86 %, and 7.87 % while the highest RMSD values are 0.01×10^{-3}, 0.005×10^{-3}, and 4.37×10^{-3} for the van't Hoff, λh, and modified Apelblat models, respectively. In ACN-water mixtures the highest RAD % values obtained are 11.51 %, 11.64 % and 8.25 %, while the highest RMSD values are 0.13×10^{-3}, 0.05×10^{-3} and 0.58×10^{-3} respectively. Lastly, with the mixtures of DMF and water, the highest RAD % values obtained are 18.55 %, 21.08 % and 17.05 %, while the highest RMSD values are 0.4×10^{-3}, 2.42×10^{-3} and 0.58×10^{-3} for the three models, respectively.

The experimental solubility data at each solvent composition were plotted individually over the eight studied temperatures and compared with the corresponding solubility values calculated using the modified Apelblat equation. The fitted results exhibit good agreement with the experimental data across all solvent compositions. The corresponding individual comparison plots are presented in the supplementary section (Figures S2–S17). Overall, the modified Apelblat equation shows slightly better agreement with the experimental data; however, all three models provide comparable fits. The similar order of magnitude of the RAD and RMSD values indicates that even the simpler van't Hoff equation is capable of describing the solubility data reasonably well across the studied solvent systems.

Table 7
Values of parameters obtained using solubility models for 4-HC in different (ACN + water) mixed solvents.

x_{ACN}	van't Hoff equation				
	a/K	b	RMSD×10^3	RAD×10^2	
0.00	4.7762	-4281.08	0.01	9.80	
0.20	-0.7666	-2146.23	0.03	4.46	
0.40	3.8065	-3268.02	0.13	11.51	
0.60	4.5890	-2939.98	0.51	8.72	
0.80	6.7974	-3290.58	1.32	5.63	
1.00	6.6035	-3529.92	0.85	7.82	
x_{ACN}	λh equation				
	λ	h	RMSD×10^3	RAD×10^2	
0.00	0.02	247,764.67	0.005	9.86	
0.20	0.0036	523,320.66	0.01	4.36	
0.40	0.0485	65,881.73	0.05	11.64	
0.60	0.2038	14,003.60	0.18	8.70	
0.80	1.0152	3230.22	0.47	5.62	
1.00	0.4883	7142.84	0.30	7.79	
x_{ACN}	Apelblat equation				
	A	B/K	C	RMSD×10^3	RAD×10^2
0.00	1177.30	-57,487.38	-174.46	0.00	2.67
0.20	-583.08	24,277.81	86.64	0.01	2.20
0.40	1139.74	-54,814.08	-169.01	0.05	4.87
@#@	601.22	-30,013.83	-88.77	0.58	8.25
0.80	-509.38	20,132.55	76.80	1.01	3.90
1.00	-229.29	7174.31	35.10	0.78	

Correlations explored herein proved to be valid for actual application to industrial design and operation. Consequently, experimental information and the constructed correlation models are crucial reference points and convenient simulation tools to improve the efficiency of the separation and purification of the industrial process of 4-HC.

4. Conclusions

This work provides new solubility data for 4-hydroxycoumarin in pure along with DMSO–water, ACN–water, and DMF–water mixtures over the temperature range 288.15–323.15 K, which have not been previously reported. In all solvent systems, the solubility of 4-HC increased with temperature. The experimental results were correlated using the van't Hoff model, the modified Apelblat equation, and the λh equation. Although the modified Apelblat equation showed marginally better performance, the similar total RAD values across models suggest that the simpler van't Hoff equation is equally capable of representing the data.

For the first time, the solubility behaviour of 4-HC has been systematically evaluated across a wide range of aqueous–organic solvent compositions at eight temperatures. The results show that at every temperature studied, the solubility of 4-HC in aqueous–organic mixtures was significantly higher than in pure water. The ACN-water and pure ACN solvent systems exhibited the lowest solubility, among the pure organic solvents (DMF, DMSO, and ACN), whereas pure DMF provided highest solubility. Overall, the solubility trend in the pure solvents followed the order: DMF > DMSO > ACN > H_2O.

Compared with previous solubility studies on compounds such as

mirtazapine, sulfamethazine and naringin where solubility enhancement often required specific co-solvent ratios or polymeric/surfactant additives [47–49], this study demonstrates a sustained increase in solubility across all tested aqueous-organic mixtures without additional solubilizing agents. The experimental solubility dataset and derived thermodynamic correlation parameters presented here support improved solvent selection and facilitate the design, optimization, and scale-up of 4-HC related processes. These findings are expected to be valuable for extraction, purification, and formulation strategies involving this compound.

CRediT authorship contribution statement

Sintu Ganai: Writing – review & editing, Writing – original draft, Supervision, Funding acquisition, Formal analysis, Data curation, Conceptualization. **Bidhan Chandra Mahatha:** Investigation, Formal analysis, Data curation. **Avishek Saha:** Investigation, Formal analysis, Data curation. **Jit Chakraborty:** Visualization, Investigation, Formal analysis. **Puspal Mukherjee:** Validation, Software, Methodology, Conceptualization. **Pratima Mandal:** Investigation, Formal analysis, Data curation. **Adel Noubigh:** Writing – review & editing, Software, Conceptualization. **Sanjay Roy:** Writing – review & editing, Writing – original draft, Supervision, Software, Resources, Conceptualization.

Declaration of competing interest

We declare no conflict of interest.

Acknowledgments

Sintu Ganai thanks Netaji Subhas Open University for funding the video project grant number Reg/0525 dated 07.06.2024. The authors extend their appreciation to the Deanship of Scientific Research at Northern Border University, Arar, KSA for funding this research work through the project number (NBU-FFR-2026-1497-02).

Supplementary materials

Supplementary material associated with this article can be found, in the online version, at doi:10.1016/j.ctta.2026.100272.

Data availability

Data will be made available on request.

References

[1] G.L. Perlovich, A. Bauer-Brandl, Pharm. Res 20 (3) (2003) 471–478, https://doi.org/10.1023/A:1022624725495.
[2] E. Sheikholeslamzadeh, S. Rohani, Ind Eng Chem Res 51 (1) (2012) 464–473, https://doi.org/10.1021/ie201344k.
[3] S.G. Johnsen, Fluid Ph. Equilib 556 (2022) 113380, https://doi.org/10.1016/j.fluid.2022.113380.
[4] G. Kher, H. Ram, D. Kundariya, P. Ambasana, R. Tandel, R. Ghumara, B. Dodiya, C. Patel, R. Bhola, Discov. Chem. 1 (1) (2024) 40, https://doi.org/10.1007/s44371-024-00044-4.
[5] N. Dhayananth, S. Karthika, P. Kalaichelvi, T.K. Radhakrishnan, J Chem Thermodyn 170 (2022) 106777, https://doi.org/10.1016/j.jct.2022.106777.
[6] G. Zhou, J. Dong, Z. Wang, Z. Li, Q. Li, B. Wang, J Mol Liq 265 (2018) 442–449, https://doi.org/10.1016/j.molliq.2018.06.035.
[7] X. Li, Y. Liu, Y. Cao, Y. Cong, A. Farajtabar, H. Zhao, J. Chem. Eng. Data 63 (6) (2018) 2219–2227, https://doi.org/10.1021/acs.jced.8b00179.
[8] J. Kaur, P. Famta, N. Khurana, M. Vyas, G.L. Khatik, New and future developments in microbial biotechnology and bioengineering, Elsevier (2020) 209–218, https://doi.org/10.1016/B978-0-12-821006-2.00016-9.
[9] Y. Bingwei, S. Joyce, D.C J, 4-hydroxy coumarin deriv. (1998). https://www.surechembl.org/document/US-5985912-A.
[10] S.M. Banday, M. Showkat, K.Z. Khan, Asian J. Pharm. Pharmacol. 5 (3) (2019) 470–479, https://doi.org/10.31024/ajpp.2019.5.3.7.
[11] K. Majumdar, B. Sinha, I. Ansary, S. Ganai, D. Ghosh, B. Roy, B. Sridhar, Synth. (Mass) 46 (13) (2014) 1807–1814, https://doi.org/10.1055/s-0033-1341027.
[12] K. Majumdar, S. Ganai, B. Chattopadhyay, K. Ray, Synlett 2011 (16) (2011) 2369–2373, https://doi.org/10.1055/s-0030-1260312.
[13] S. Ganai, B.C. Mahatha, A. Saha, J. Chakraborty, P. Alam, P. Mukherjee, H. Shaikh, D. Mallick, S. Roy, J Mol Liq 432 (2025) 127692, https://doi.org/10.1016/j.molliq.2025.127692.
[14] J. Chakraborty, K. Mahali, A.M.A. Henaish, J. Ahmed, S.M. Alshehri, S. Roy, Biophys. Chem 309 (2024) 107229, https://doi.org/10.1016/j.bpc.2024.107229.
[15] N. Sing, P. Mondal, M. Mondal, K. Mahali, A.M.A. Henaish, B. Saha, J. Ahmed, A. Hussain, S. Roy, Chem Phys Lett 831 (2023) 140847, https://doi.org/10.1016/j.cplett.2023.140847.
[16] C.F. Trujillo-Trujillo, F. Angarita-Reina, M. Herrera, C.P. Ortiz, R.E. Cardenas-Torres, F. Martinez, D.R. Delgado, Liquids 3 (1) (2022) 7–18, https://doi.org/10.3390/liquids3010002.
[17] Z.J. Cárdenas, D.M. Jiménez, O.A. Almanza, A. Jouyban, F. Martínez, W.E. Acree, Phys. Chem. Liq. 56 (4) (2018) 465–481, https://doi.org/10.1080/00319104.2017.1346651.
[18] A.H. Shah, S.M.R. Islam, M.D. Albaqami, T. Hasan, D. Kumar, S.M. Wabaidur, M. Z. Ansari, Md.A. Hoque, D.M.S. Islam, M. Kabir, RSC Adv 14 (9) (2024) 5981–5993, https://doi.org/10.1039/D3RA07493E.
[19] A.L.R. Silva, M.J.S. Monte, V.M.F. Morais, M.D.M.C. Ribeiro da Silva, J Chem Thermodyn 74 (2014) 67–77, https://doi.org/10.1016/j.jct.2014.04.001.
[20] D. Kumar, J.M. Khan, M. Posa, ChemistrySelect 10 (24) (2025), https://doi.org/10.1002/slct.202405789.
[21] S. Akay, B. Kayan, A. Jouyban, F. Martínez, W.E. Acree, J Mol Liq 339 (2021) 116761, https://doi.org/10.1016/j.molliq.2021.116761.
[22] K.M. Anis-Ul-Haque, M.A.A. Hossain, N. Uddin, Md. Jonayed, M.K. Gatasheh, D. Kumar, M.A. Goni, Md.T.R. Joy, Md.A. Hoque, Colloids Surf. A: Physicochem. Eng. Asp. 692 (2024) 133972, https://doi.org/10.1016/j.colsurfa.2024.133972.
[23] Ahmed, B., Khan, J.M., Mahbub, S., M. Shahadat, H., Kumar, D., Banjare, M. K., Hasan, T., Rana, S., & Hoque, Md.A. (2024). *Colloid Polym Sci*, 302(12), 1939–1956. https://doi.org/10.1007/s00396-024-05317-z.
[24] A. Saha, K. Mahali, S. Roy, Can J Chem 101 (8) (2023) 548–556, https://doi.org/10.1139/cjc-2022-0308.
[25] S. Ganai, P. Mukherjee, K. Mahali, A. Saha, A. Hossain, A.v. Soldatov, A.M. A. Henaish, J. Ahmed, S. Roy, New J. Chem. 47 (28) (2023) 13547–13557, https://doi.org/10.1039/D3NJ02412A.
[26] A. Saha, J. Chakrabortya, Abdelmageed. Abualreish, S. Kundu, K. Mahali, S. Ganai, P. Mukherjee, S. Roy, Phys. Chem. Res. 12 (4) (2024) 1049–1064, https://doi.org/10.22036/pcr.2024.460474.2533.
[27] A. Saha, K. Mahali, P. Mukherjee, S. Ganai, A. Hossain, A.M.A. Henaish, S. Roy, Chem Phys Lett 828 (2023) 140719, https://doi.org/10.1016/j.cplett.2023.140719.
[28] A. Saha, K. Mahali, P. Mukherjee, S. Ganai, A. Hossain, A.M.A. Henaish, S. Kundu, J. Ahmed, S. Roy, J Mol Liq 389 (2023) 122852, https://doi.org/10.1016/j.molliq.2023.122852.
[29] A. Saha, K. Mahali, S. Ganai, P. Mukherjee, N.K. Shrestha, A.M.A. Henaish, J. Ahmed, S. Kundu, S. Roy, J Mol Liq 391 (2023) 123352, https://doi.org/10.1016/j.molliq.2023.123352.
[30] M. Khorsandi, E. Nemati-Kande, F. Hosseini, F. Martinez, H. Shekaari, M. Mokhtarpour, J Mol Liq 68 (2023) 120650, https://doi.org/10.1016/j.molliq.2022.120650.
[31] N. Sing, K. Mahali, P. Mondal, J. Chakraborty, A.M.A. Henaish, J. Ahmed, A. Hussain, S. Roy, Biophys. Chem 306 (2024) 107154, https://doi.org/10.1016/j.bpc.2023.107154.
[32] Y. Marcus, Ion Solvation, 7th Edition, Wiley, New York, 1985.
[33] Sk. Imran, A. Hossain, K. Mahali, P.S. Guin, A. Datta, S. Roy, J Mol Liq 302 (2020) 112566, https://doi.org/10.1016/j.molliq.2020.112566.
[34] A. Saha, S. Ghosh, S. Ganai, P. Mukherjee, K. Mahali, B. Saha, A.M.A. Henaish, P. S. Guin, P. Alam, S. Roy, Biophys. Chem 307 (2024) 107195, https://doi.org/10.1016/j.bpc.2024.107195.
[35] A. Hossain, S. Roy, S. Ghosh, S. Mondal, B.K. Dolui, RSC Adv 5 (85) (2015) 69839–69847, https://doi.org/10.1039/C5RA12403D.
[36] R.D. Nelson, D.R. Lide, A.A. Maryott, Selected Values of Electric Dipole Moments For Molecules in the Gas Phase, U. S. National Bureau of Standards, 1967, https://doi.org/10.6028/NBS.NSRDS.10.
[37] B.V. Kumar Naidu, K.C. Rao, M.C.S. Subha, J. Chem. Eng. Data 47 (3) (2002) 379–382, https://doi.org/10.1021/je0101395.
[38] J.F. Coetzee, G.R. Padmanabhan, J Phys Chem 66 (9) (1962) 1708–1713, https://doi.org/10.1021/j100815a036.
[39] K. Mahali, S. Roy, B.K. Dolui, J Solut. Chem 42 (5) (2013) 1096–1110, https://doi.org/10.1007/s10953-013-0005-y.
[40] Y. Li, F. Wang, L. Xu, H. Jin, B. Ren, Fluid Ph. Equilib 298 (2) (2010) 246–252, https://doi.org/10.1016/j.fluid.2010.08.006.
[41] A. Fathi-Azarbayjani, M. Abbasi, J. Vaez-Gharamaleki, A. Jouyban, J Mol Liq 215 (2016) 339–344, https://doi.org/10.1016/j.molliq.2015.12.005.
[42] A. Apelblat, E. Manzurola, J Chem Thermodyn 31 (1) (1999) 85–91, https://doi.org/10.1006/jcht.1998.0424.
[43] A. Apelblat, E. Manzurola, J Chem Thermodyn 29 (12) (1997) 1527–1533, https://doi.org/10.1006/jcht.1997.0267.
[44] E. Manzurola, A. Apelblat, J Chem Thermodyn 34 (7) (2002) 1127–1136, https://doi.org/10.1006/jcht.2002.0975.
[45] A. Książczak, J.J. Kosinski, Fluid Ph. Equilib 44 (2) (1988) 211–236, https://doi.org/10.1016/0378-3812(88)80112-2.
[46] A. Ksiazczak, K. Moorthi, I. Nagata, Fluid Ph. Equilib 95 (1994) 15–29, https://doi.org/10.1016/0378-3812(94)80058-8.

[47] H. Matsuda, M. Kosuge, R. Yoshimura, Y. Naito, T. Tsuji, K. Kurihara, K. Tochigi, J Solut. Chem 54 (5) (2025) 626–640, https://doi.org/10.1007/s10953-025-01442-7.
[48] K.E. Ezealisiji, C.J. Mbah, P.O. Osadebe, Pharmacol. Pharm. 06 (10) (2015) 471–476, https://doi.org/10.4236/pp.2015.610049.
[49] D.I. Caviedes-Rubio, C. Buendía-Atencio, R.E. Cardenas-Torres, C.P. Ortiz, F. Martinez, D.R. Delgado, Molecules 30 (17) (2025) 3590, https://doi.org/10.3390/molecules30173590.